Received: 31 January 2019 | Revised: 22 July 2019 | Accepted: 28 July 2019

DOI: 10.1111/pce.13639

ORIGINAL ARTICLE

WILEY Plant, Cell & Environment

No evidence for triose phosphate limitation of light-saturated leaf photosynthesis under current atmospheric CO_2 concentration

Dushan P. Kumarathunge[1,2] | Belinda E. Medlyn[1] | John E. Drake[1,3] | Alistair Rogers[4] | Mark G. Tjoelker[1]

[1] Hawkesbury Institute for the Environment, Western Sydney University, Penrith, NSW 2751, Australia

[2] Plant Physiology Division, Coconut Research Institute of Sri Lanka, Lunuwila, 61150, Sri Lanka

[3] Forest and Natural Resources Management, College of Environmental Science and Forestry, State University of New York, Syracuse, NY 13210, USA

[4] Environmental and Climate Sciences Department, Brookhaven National Laboratory, Upton, NY 11973, USA

Correspondence
D. P. Kumarathunge, Plant Physiology Division, Coconut Research Institute of Sri Lanka, Lunuwila, 61150, Sri Lanka.
Email: dkumarathunge@gmail.com

Funding information
Brookhaven National Laboratory, Grant/Award Numbers: DE-SC0012704 and DE-SC0012704; Western Sydney University International PhD Scholarship

Abstract

The triose phosphate utilization (*TPU*) rate has been identified as one of the processes that can limit terrestrial plant photosynthesis. However, we lack a robust quantitative assessment of *TPU* limitation of photosynthesis at the global scale. As a result, *TPU*, and its potential limitation of photosynthesis, is poorly represented in terrestrial biosphere models (TBMs). In this study, we utilized a global data set of photosynthetic CO_2 response curves representing 141 species from tropical rainforests to Arctic tundra. We quantified *TPU* by fitting the standard biochemical model of C_3 photosynthesis to measured photosynthetic CO_2 response curves and characterized its instantaneous temperature response. Our results demonstrate that *TPU* does not limit leaf photosynthesis at the current ambient atmospheric CO_2 concentration. Furthermore, our results showed that the light-saturated photosynthetic rates of plants growing in cold environments are not more often limited by *TPU* than those of plants growing in warmer environments. In addition, our study showed that the instantaneous temperature response of *TPU* is distinct from temperature response of the maximum rate of Rubisco carboxylation. The new formulations of the temperature response of *TPU* derived in this study may prove useful in quantifying the biochemical limits to terrestrial plant photosynthesis and improve the representation of plant photosynthesis in TBMs.

KEYWORDS

A/C_i curves, C_3 photosynthesis, maximum carboxylation capacity, potential electron transport rate, temperature, terrestrial biosphere models

1 | INTRODUCTION

Terrestrial biosphere models (TBMs) are one of the principal tools used to estimate the impact of climate change on terrestrial vegetation (Medlyn et al., 2011; Mercado et al., 2018; Rogers, Serbin, et al., 2017). Plant photosynthesis is one of the key components in these models. Robust representation of photosynthesis and its response to climate change are important for predicting the response of terrestrial vegetation to global change. Many TBMs incorporate the Farquhar, von Caemmerer, and Berry (1980) biochemical model of C_3 photosynthesis (FvCB hereafter) to estimate terrestrial gross primary productivity (GPP; Rogers, Medlyn, et al., 2017). Hence, the effect of climate change on modelled GPP depends on the formulation and parameterization of the FvCB model, and in particular, on the sensitivity of the key model parameters to environmental variables such as temperature, atmospheric CO_2 concentration, and soil moisture (Smith & Dukes, 2013).

The FvCB model mechanistically represents photosynthetic CO_2 assimilation as the minimum of two biochemical processes: Rubisco carboxylation and ribulose-1,5-bisphosphate (RuBP) regeneration (Von Caemmerer, 2013; Farquhar et al., 1980). However, under some environmental conditions, a third biochemical process, the triose phosphate utilization (*TPU*) rate, limits net photosynthesis (Harley & Sharkey, 1991; McClain & Sharkey, 2019; Sharkey, 1985; Sharkey, Bernacchi, Farquhar, & Singsaas, 2007). Decades of empirical research have sought to improve the model representation of the first two processes (Hikosaka, Ishikawa, Borjigidai, Muller, & Onoda, 2006; Kattge & Knorr, 2007; Kumarathunge et al., 2019, Medlyn et al., 2002; Rogers, Medlyn, et al., 2017; Wullschleger, 1993). In contrast, *TPU* is often ignored when parameterizing the FvCB model (Crous et al., 2013; De Kauwe et al., 2016; Manter & Kerrigan, 2004; Vårhammar et al., 2015) and is rarely implemented in TBMs (Kattge, Knorr, Raddatz, & Wirth, 2009; Smith, Lombardozzi, Tawfik, Bonan, & Dukes, 2017; Smith, Malyshev, Shevliakova, Kattge, & Dukes, 2016). Although we have a sound biochemical understanding of the *TPU* limitation on plant photosynthesis (Sharkey, 1985), we lack a robust quantitative assessment of *TPU* limitation of photosynthesis at the global scale. There is a dearth of empirical evidence of environmental controls on *TPU* limitation across different plant functional types and biomes (Lombardozzi et al., 2018) that is a critical knowledge gap limiting informed implementation of TBM formulations that include *TPU* limitation as part of the FvCB model (Rogers, Medlyn, et al., 2017).

Empirical studies demonstrate that *TPU* limitation occurs more frequently at higher CO_2 concentration (Busch & Sage, 2017; Labate & Leegood, 1988; Sage, Sharkey, & Seemann, 1989), but it is not clear to what extent it limits photosynthesis at current or future predicted atmospheric CO_2 concentrations. Some studies indicate that net photosynthesis is more likely to be *TPU* limited at low temperatures even under ambient CO_2 concentrations (Busch & Sage, 2017; Sage & Sharkey, 1987; Stitt & Hurry, 2002; Strand, Hurry, Gustafsson, & Gardeström, 1997; Yang, Preiser, Li, Weise, & Sharkey, 2016), but it is not clear how widespread this finding might be. At low temperatures, due to lower activity of proteins of the sucrose synthesis pathway (e.g., cytosolic fructose-1,6-bisphosphatase and sucrose phosphate synthase), the rate of triose phosphate production in the Calvin cycle cannot be met by the capacity of sucrose synthesis (Pons, 2012). Due to this overproportional decrease in sucrose synthesis, it can be expected that *TPU* limitation would be more frequent at low temperatures (Sharkey et al., 1986; Stitt, Grosse, & Woo, 1988). Hence, it can be hypothesized that TPU limitation of photosynthesis is more prevalent in plants growing at cold environments compared with the plants grown at warm environments. Nevertheless, several lines of evidence suggested that sucrose synthesis capacity is increased as the plants acclimate to low temperatures (Stitt & Hurry, 2002). Also, previous literature suggested that plants regulate *TPU*, Rubisco activity, and RuBP regeneration so that the capacity to fix carbon will not exceed the capacity to make sugars (Stitt et al., 1988; Stitt & Grosse, 1988). Further, plants maintain *TPU* rate just slightly higher than what is likely to be required (Yang et al., 2016). Hence, it is also likely that photosynthesis of cold acclimated plants is less likely to be limited by *TPU* as has been observed previously in a limited number of species (Sage & Sharkey, 1987). However, it is not clear to what extent that *TPU* limits photosynthesis in plants growing in the diverse range of different growth temperatures that are represented by TBMs. Most studies on *TPU* limitation have been conducted under controlled experimental conditions (Bernacchi et al., 2013). Evidence for the occurrence of *TPU* limitation in mature plants in natural ecosystems is rare (Ellsworth, Crous, Lambers, & Cooke, 2015). Owing to this lack of evidence, many TBMs either do not consider *TPU* limitation or represent it nonmechanistically (Rogers, Medlyn, et al., 2017; Lombardozzi et al., 2018). For example, some models assume *TPU* to be a fixed fraction of the maximum rate of Rubisco carboxylation (V_{cmax}), where $W_p = 0.5V_{cmax}$ (Clark et al., 2011,Oleson et al 2013; Collatz, Ball, Grivet, & Berry, 1991). Moreover, these models assume that the temperature response of *TPU* is identical to that for V_{cmax} (e.g., Oleson et al., 2013). Studies of the temperature response of *TPU* are also rare (Yang et al., 2016), so there are limited resources available to inform the adoption of an independent *TPU* temperature response in TBMs.

Recently, Lombardozzi et al. (2018) examined the effect of including *TPU* limitation in the Community Land Model (CLM) v4.5. They found that implementation of *TPU* in CLM resulted in a limitation of photosynthesis by *TPU* under present day and future predicted ambient CO_2 concentrations, most consistently at high latitudes, and an approximate 6% reduction in terrestrial carbon uptake and storage at the end of the 21st century. To represent *TPU*, the following assumptions were made. First, *TPU* was assumed to be a fixed fraction of V_{cmax}. Second, the temperature response of *TPU* was assumed to be the same as for V_{cmax}. Thermal acclimation of *TPU* was assumed to be the same as that of V_{cmax}, which was represented by an algorithm derived from empirical data (Kattge & Knorr, 2007). Owing to the limitations of that empirical data set, the algorithm does not allow for temperature acclimation below 11°C or above 29°C. Lombardozzi et al. (2018) highlighted the need for improved physiological understanding of the conditions under which *TPU* limitation might be important and the need for empirically informed implementation of *TPU* in TBMs. However, to date, there is no comprehensive study available in the literature that can enable an assessment of *TPU* in response to the environment. Therefore, the validity of the above assumptions, and similar ones in other TBMs (Rogers, Medlyn, et al., 2017; Smith & Dukes, 2013), remains uncertain. Given the sensitivity of terrestrial plant photosynthesis to *TPU* in current TBMs, as highlighted by Lombardozzi et al. (2018), it is important to synthesize the extent of *TPU* limitation and its temperature response using data obtained across different ecosystems at the global scale.

To address this knowledge gap, we used a global data set of plant photosynthetic CO_2 response curves spanning ecosystems from tropical rainforests to Arctic tundra. We inferred key photosynthetic biochemical parameters by fitting a standard C_3 photosynthesis model to the raw gas exchange data. Our primary objective was to improve the current understanding of *TPU* limitation on leaf net photosynthesis by describing and summarizing the extent of *TPU* limitation across important plant functional types grown and measured in their natural

environments around the globe. In particular, we examined the following three questions: (a) Is *TPU* limitation to leaf photosynthesis widespread at current ambient atmospheric CO_2 concentrations? (b) Is the photosynthetic rate of plants growing in cold environments more often limited by *TPU* than in plants growing in warmer environments? And (c) do *TPU* and V_{cmax} have similar instantaneous temperature responses?

2 | MATERIALS AND METHODS

2.1 | Data sources

We used AC_i-TGlob_V1.0 (Kumarathunge et al., 2018), a global data set of plant photosynthetic CO_2 response curves (referred to as A/C_i curves hereafter), for this analysis. The data set contains a total of 5,113 A/C_i curves measured in situ at multiple leaf temperatures of upper canopy sun-lit leaves from 141 plant species from 42 different studies conducted around the world (Table S1). The data set covers diverse ecosystems including tropical rainforests, temperate and boreal forests, semiarid woodlands, and Arctic tundra. A detailed description of data collection, data compilation, and quality control is given in Kumarathunge et al. (2018).

2.2 | Theory

We used the Farquhar et al. (1980) C_3 photosynthesis model to infer the biochemical limitations on net leaf photosynthesis (A_{net}). The model incorporates three principal processes occurring in plant leaves at the same time: photosynthesis, photorespiration, and mitochondrial respiration in the light (Farquhar et al., 1980). The original FvCB model represents A_{net} as the minimum of two process rates: the Rubisco carboxylation-limited photosynthetic rate (W_c) and the RuBP regeneration-limited photosynthetic rate (W_j), and later revised to include the TPU-limited rate, W_p (Harley & Sharkey, 1991; Sharkey, 1985). The widely used formulation of the model is as follows:

$$A_{net} = \min(W_c, W_j, W_p)\left(1 - \frac{\Gamma^*}{C_i}\right) - R_L \quad (1)$$

$$W_c = V_{cmax}\frac{C_i}{C_i + K_c\left(1 + \frac{O_i}{K_o}\right)} \quad (2)$$

$$W_j = \frac{J}{4}\frac{C_i}{\left(C_i + 2\Gamma^*\right)} \quad (3)$$

$$W_p = \frac{3TPU\ C_i}{C_i - (1 + 3\alpha)\Gamma^*}, \quad (4)$$

where V_{cmax} is the maximum rate of carboxylation by the enzyme RuBP carboxylase–oxygenase (Rubisco), C_i and O_i (μmol mol^{-1}) are intercellular CO_2 and O_2 concentrations, respectively, K_c and K_o (μmol mol^{-1}) are Michaelis–Menten coefficients of Rubisco activity for CO_2 and O_2, respectively, Γ^* (μmol mol^{-1}) is the CO_2 compensation point in the absence of photorespiration, R_L (μmol m^{-2} s^{-1}) is the nonphotorespiratory CO_2 evolution in the light, J (μmol m^{-2} s^{-1}) is the rate of electron transport that is related to incident photosynthetically active photon flux density (Q, μmol m^{-2} s^{-1}) by Equation (5), *TPU* (μmol m^{-2} s^{-1}) is the TPU rate, and α is the fraction of the photorespiratory product, glycolate, returned to the chloroplast. We assumed α = 0 (a closed photorespiratory cycle; Harley & Sharkey, 1991) when fitting A/C_i curves.

$$\theta J^2 - (\phi Q + J_{max})J + \phi Q J_{max} = 0, \quad (5)$$

where J_{max} (μmol m^{-2} s^{-1}) is the potential rate of electron transport, ϕ (μmol mol^{-1}) is the quantum yield of electron transport, and θ (dimensionless) is the curvature of the light response curve.

We fitted Equations (1)–(5) to each measured A/C_i curve using the *fitacis* function within the plantecophys package (Duursma, 2015) in R version 3.5.1 (R Development Core Team, 2018). The model fitting algorithm is based on the logic introduced by (Gu, Pallardy, Tu, Law, & Wullschleger, 2010). Fitting is done by looping over the potential limitation states. The different limitation states are obtained by assigning each point in an A/C_i curve to one of three limitations, without a prior assumption in the order of each limitation states occur. Parameter values are obtained for each limitation state by regression. Parameter values are retained for the limitation state yielding the best overall fit with minimum sum of squares error (Duursma, 2015). This fitting approach is appropriate because it makes no a priori assumptions about the limitation states at different parts of the curve. Some curves may show no *TPU* limitation. We used the Bernacchi, Singsaas, Pimentel, Portis, and Long (2001) kinetic constants for the temperature response of K_c, K_o, and Γ^* as given in Medlyn et al. (2002). We used measured photosynthetically active irradiance values for fitting A/C_i curves whenever available, otherwise assuming a fixed value of 1,800 μmol m^{-2} s^{-1}. We assumed default *fitacis* parameter values for quantum yield of electron transport, Φ (0.24 mol mol^{-1}), and the curvature of the light response curve, θ (0.85; unitless), for all data sets (Equation 5). In our A/C_i curve fitting method, we did not account for the variations in mesophyll conductance (g_m) as g_m is not separately identifiable from V_{cmax} when fitting an A/C_i curve. Therefore, the estimated parameters, V_{cmax} and J_{max}, are considered apparent values (Bahar, Hayes, Scafaro, Atkin, & Evans, 2018). This approach is appropriate for this analysis because almost all current TBMs ignore g_m and use apparent V_{cmax} and J_{max} values. We did not account for CO_2 and H_2O diffusion through cuvette gaskets as there was insufficient information to implement those corrections accurately across the large set of curves. We visually inspected every fitted A/C_i curve in the data set for possible outliers and erroneous data points (i.e., negative intercellular CO_2 concentrations). We excluded parameters of a given A/C_i curve from further analysis if the r^2 of the fitted function was less than.90 (De Kauwe et al., 2016). This criterion removed approximately 6% of the total A/C_i curves of the data set. After screening, the data set contained a total of 4,260 A/C_i curves measured at leaf

temperatures ranging from 3°C to 50°C. A detailed description of the A/C_i curve fitting and parameter quality control can be found in Kumarathunge et al. (2018).

We utilized the intercellular CO_2 concentration at the rate transition points to infer the biochemical process that limits the net photosynthetic rate at current ambient CO_2 levels (400 μmol mol^{-1}). The C_i transition points between W_c and W_j ($C_{i\text{-}1}$) and W_j and W_p ($C_{i\text{-}2}$) were located by identifying the points at which the two functions (i.e., either W_c and W_j or W_j and W_p) intersect (see Figure 1). We calculated the C_i corresponding to the current ambient CO_2 concentration of 400 μmol mol^{-1} by assuming a constant C_i:C_a of 0.7 (median C_i:C_a across the data set; Figure S1), giving C_i = 280 μmol mol^{-1}. Under these assumptions, we inferred that the photosynthetic rate at the current ambient CO_2 concentration is W_c limited if $280 \leq C_{i\text{-}1}$ and $C_{i\text{-}2}$, W_j limited if $C_{i\text{-}1} < 280 \leq C_{i\text{-}2}$, and W_p limited if $C_{i\text{-}1}$ and $C_{i\text{-}2} \leq 280$. A conceptual depiction of these conditions is shown in Figure 1.

2.3 | Data analysis

The data set utilized in this study contains data measured across a range of experiments including mature plants growing in their native environments, common garden studies, and data sets with repeated seasonal photosynthetic measurements. Our objective was to summarize the extent of *TPU* limitation on leaf photosynthesis across the globe. First, we utilized all available data to quantify how frequently *TPU* is limiting at the current ambient CO_2 concentration. Second, we utilized a subset of the data set that contains measurements from mature plants growing and measured in their native environments to identify patterns in *TPU* limitation across different ecosystems. To examine temperature responses of *TPU*, we further subset the data to only consider curves where *TPU* limitation was identified by the fitting algorithm. The temperature response of *TPU* was fitted using the peaked Arrhenius function (Johnson, Eyring, & Williams, 1942):

$$TPU_{(T_k)} = TPU_{25} \exp\left[\frac{E_a(T_k - 298.15)}{(298.15\, R\, T_k)}\right] \frac{1 + \exp\left(\frac{298.15\, \Delta S - H_d}{298.15\, R}\right)}{1 + \exp\left(\frac{T_k\, \Delta S - H_d}{T_k\, R}\right)}, \quad (6)$$

where $TPU_{(T_k)}$ is the process rate at a given temperature, T_k (K), TPU_{25} is the TPU rate at 25°C, R is the universal gas constant (8.314 J mol^{-1} K^{-1}), E_a (kJ mol^{-1}) is the activation energy term that describes the exponential increase in the temperature response function with the

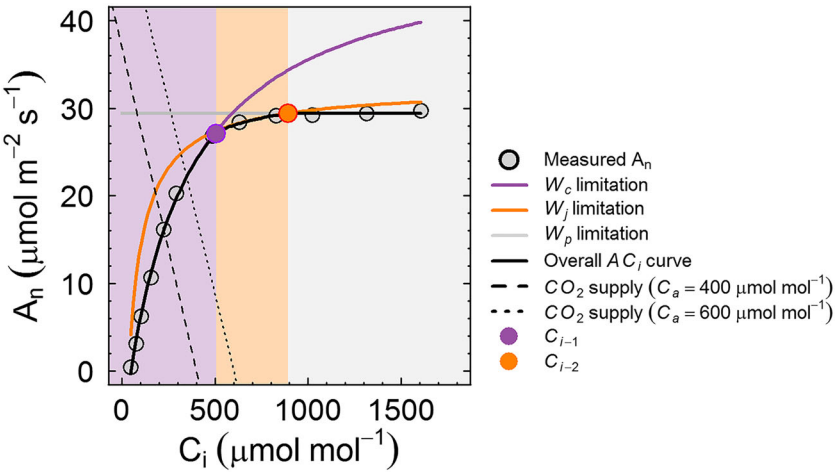

FIGURE 1 Conceptual figure demonstrating the typical CO_2 response of leaf net photosynthesis (A/C_i curve). Filled circles depict the measured leaf net photosynthetic rated at different intercellular CO_2 concentration levels (C_i). Solid lines depict the Rubisco carboxylation-limited photosynthetic rate (W_c limitation, purple line), RuBP regeneration-limited photosynthetic rate (W_j limitation, orange line), triose phosphate utilization-limited rate (W_p limitation, grey line), and the limiting rate of net photosynthesis (black). The two filled circles depict the C_i at transition points from Rubisco carboxylation-limited photosynthetic rate to RuBP regeneration-limited photosynthetic rate ($C_{i\text{-}1}$, purple circle) and from RuBP regeneration-limited photosynthetic rate to *TPU*-limited photosynthetic rate ($C_{i\text{-}2}$, orange circle). The dashed and dotted lines depict the CO_2 supply functions corresponding to current ambient CO_2 concentration (400 μmol mol^{-1}, dashed line) and an elevated CO_2 concentration (600 μmol mol^{-1}, dotted line). The background-shaded area depicts the C_i range where net photosynthesis is limited by W_c (purple), W_j (orange), and W_p (grey). The data shown in this figure were obtained at a leaf measurement temperature of 18°C on *Eucalyptus parramattensis* trees grown in whole tree chambers in Richmond, NSW, Australia. The fitted parameter values were V_{cmax} = 155, J_{max} = 250, *TPU* = 11, and R_{day} = 3.1 μmol m^{-2} s^{-1}

increase in temperature, H_d (kJ mol^{-1}) is the deactivation energy, and ΔS (J mol^{-1} K^{-1}) is the entropy term. To avoid overparameterization, we assumed a fixed value of 200 kJ mol^{-1} for H_d in Equation (6) for all data sets (Dreyer et al., 2001). Parameters of Equation (6) were estimated in a non-linear mixed model framework (Zuur et al., 2009) using the *nlme* function within the *nlme* package in R version 3.5.1 (R Development Core Team, 2018). We extracted the long-term (1960–1990) mean air temperature at the measurement sites using a high resolution global gridded climatology database (Hijmans, Cameron, Parra, Jones, & Jarvis, 2005). We calculated mean growing season temperature for each site as the mean temperature of the months with mean temperatures above 0°C (T_{home}). We fitted general additive models (Rigby & Stasinopoulos, 2005) to visualize the patterns in the basal rate of *TPU* (TPU_{25}) of mature plants with mean growing season temperature of the native growth environment . The R code used for the entire analysis is publicly available through the repository, https://bitbucket.org/Kumarathunge/testtpu.

3 | RESULTS

In our data set, ~32% of the A/C_i curves showed some *TPU* limitation at the upper end of the measurement intercellular CO_2 concentration range (Table 1). Arctic plants and boreal evergreen gymnosperms showed a significantly lower proportion of curves with *TPU* limitation compared with other Plant functional types (PFTs) (Table 1), whereas the PFT with the highest proportion of A/C_i curves exhibiting *TPU* limitation was the temperate evergreen angiosperms. We found no detectable correlation between leaf temperature and the C_i at process transition between W_c and W_j, either for the whole data set or for different PFTs analysed separately (Figure 2a). Similar results were observed for the C_i at the process transition between W_j and W_p (Figure 2b).

The lack of any significant correlations between C_i at process transitions and leaf temperature allowed us to utilize all available data for further inferences. When all data were pooled together, the median intercellular CO_2 concentration at the process transition between W_c and W_j ($C_{i\text{-}1}$) was 423 μmol mol^{-1} (Figure 3a). The median C_i at the process transition between W_j and W_p ($C_{i\text{-}2}$) was 810 μmol mol^{-1} (Figure 3a). Among the different PFTs, Arctic plants showed a significantly higher median $C_{i\text{-}2}$ value compared with the others (Figure 3b; post hoc Tukey tests, $P < .001$). Our data suggested that, at a current ambient atmospheric CO_2 concentration of 400 μmol mol^{-1} (i.e., C_i = 280 μmol mol^{-1}; Figure S1b), ~80% of the measured light-saturated net photosynthesis values were Rubisco carboxylation (W_c) limited. We did not observe any $C_{i\text{-}2}$ values falling below 280 μmol mol^{-1}. Hence, our study suggests that *TPU* limitation of light-saturated net photosynthesis under current ambient CO_2 concentration is extremely rare. In our data set, the median of the maximum atmospheric CO_2 concentration set point of A/C_i curve measurements was >1,400 μmol mol^{-1} for all PFTs (Table 1 and Figure S1). In all PFTs, the median of the maximum measurement C_i was higher than the median C_i that *TPU* limitation occurs (i.e., 810 μmol mol^{-1}). Hence, we emphasize that the measurement C_i range was high enough for a robust assessment of *TPU* limitation.

We investigated whether light-saturated photosynthetic rates of plants growing in cold environments are more often limited by *TPU* compared with those of plants growing in warmer environments. We observed a weak but significant negative correlation between the long-term mean growing season air temperature (T_{home}) and the C_i at process transition between W_c and W_j ($C_{i\text{-}1}$; Figure 4a; r^2 = .1).

TABLE 1 Descriptive statistics of triose phosphate utilization rate limitation across different plant functional types

Plant functional type	Total number of data sets	Total number of species	Total number of A/C_i curves	Measured maximum intercellular CO_2 concentration (μmol mol^{-1})[a]	Maximum atmospheric CO_2 concentration set point of individual A/C_i curves (μmol mol^{-1})[a]	Number of A/C_i curves showing *TPU* limitation[b] (%)
Arctic tundra	1	7	242	1,531 (1,340–1,746)	1,786 (1,772–1,915)	30 (12)
Boreal evergreen gymnosperms	5	4	429	1,348 (929–1,685)	1,800 (1,601–1,973)	71 (17)
Temperate evergreen gymnosperms	7	10	672	1,496 (1,220–1,839)	1,778 (1,102–1,909)	134 (20)
Temperate deciduous angiosperms	11	17	1,011	1,030 (897–1,832)	1,481 (1,465–1,529)	335 (33)
Temperate evergreen angiosperms	13	27	1,253	1,362 (1,039–1,744)	1767 (1747 – 1981)	591 (47)
Tropical evergreen angiosperms	6	47	653	1,227 (896–1,811)	1,747 (1,193–1,979)	209 (32)
Whole data set	43	112	4,260	1,283 (957–1,820)	1,783 (1,524–1,993)	1,370 (32)

[a]Values given are the median (2.5th and 97.5th percentiles of the distribution).

[b]Within the measurement C_i range of a given A/C_i curve.

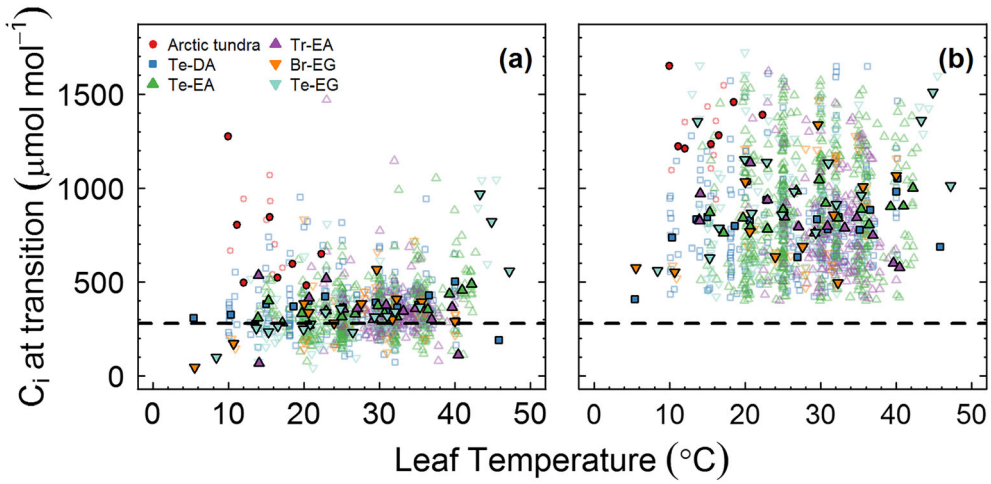

FIGURE 2 The intercellular CO_2 concentration at rate transition points as a function of leaf temperature. Panel (a) depicts the C_i at the rate transition point from Rubisco-limited photosynthesis to RuBP regeneration-limited photosynthesis ($C_{i\text{-}1}$). Panel (b) depicts the C_i at rate transition point from RuBP regeneration-limited photosynthesis to *TPU*-limited photosynthesis ($C_{i\text{-}2}$). Filled symbols show the mean of data binned in 1°C increments, and the original data are shown in the background with unfilled symbols. The horizontal broken line depicts the C_i value corresponding to current ambient atmospheric CO_2 concentration (~400 µmol mol^{-1}) at a C_i:C_a ratio of 0.7. The legend in Panel (a) depicts six different plant functional types: Arctic tundra, temperate deciduous angiosperms (Te-DA), temperate evergreen angiosperms (Te-EA), tropical evergreen angiosperms (Tr-EA), boreal evergreen gymnosperms (Br-EG), and temperate evergreen gymnosperms (Te-EG). Note that the data shown here are from the A/C_i curves that showed *TPU* limitation within the measurement C_i range (n = 1,114) [Colour figure can be viewed at wileyonlinelibrary.com]

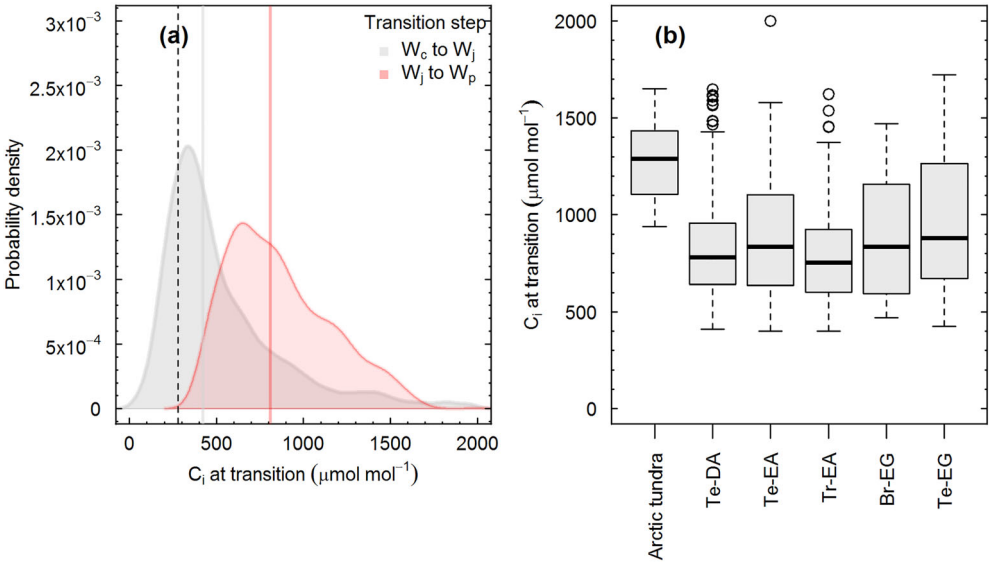

FIGURE 3 The distribution of intercellular CO_2 concentration at the rate transition point. In Panel (a), the shaded area depicts the distribution of C_i at the rate transition point from Rubisco carboxylation-limited photosynthetic rate to RuBP regeneration-limited photosynthetic rate (grey) and from RuBP regeneration-limited photosynthetic rate to *TPU*-limited photosynthetic rate (pink). The thick vertical lines in respective colours in Panel (a) show the median C_i for the two transition steps and the dashed line depicts the C_i value corresponding to the current ambient atmospheric CO_2 level (~400 µmol mol^{-1}) at a C_i:C_a of 0.7. Panel (b) shows the C_i value at the transition point from RuBP regeneration-limited photosynthesis to *TPU*-limited photosynthesis for six different plant functional types: Arctic tundra, temperate deciduous angiosperms (Te-DA), temperate evergreen angiosperms (Te-EA), tropical evergreen angiosperms (Tr-EA), boreal evergreen gymnosperms (Br-EG), and temperate evergreen gymnosperms (Te-EG). In the boxplots, the thick black line and box depict the median and interquartile range, respectively, with bars extending to 1.5 times the interquartile range. Dots outside of the box and whiskers show outlying data points [Colour figure can be viewed at wileyonlinelibrary.com]

However, we did not detect a significant correlation between T_{home} and the C_i at process transition between W_j and W_p ($C_{i\text{-}2}$; Figure 4b). The lack of a significant correlation between the $C_{i\text{-}2}$ and the plants' growth temperature strongly suggests that there is no association between the extent of the *TPU* limitation to light-saturated net photosynthesis and home climate.

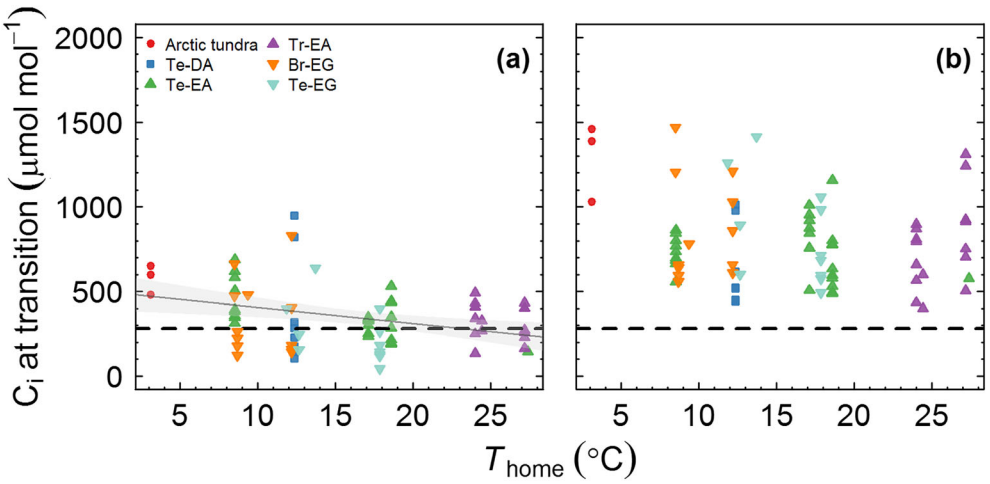

FIGURE 4 Intercellular CO_2 concentration at rate the transition point at a standard temperature of 25°C, as a function of climate of the growing environment for various plant functional types. Panel (a) depicts the C_i at the rate transition point from Rubisco carboxylation-limited photosynthetic rate to RuBP regeneration-limited photosynthesis and Panel (b) depicts the C_i at rate transition point from RuBP regeneration-limited photosynthetic rate to *TPU*-limited photosynthetic rate. The dashed lines in each panel depict the C_i value corresponding to the current ambient atmospheric CO_2 level (~400 µmol mol^{-1}) at a C_i:C_a of 0.7. The thick line in panel (a) depicts the least-squares linear regression fit ($y = 499.6 - 9.4x$; $r^2 = .1$), and the shaded area shows the 95% confidence interval of predictions. The data presented here are measurements of mature plants grown and measured in their native environments for different plant functional types: Arctic tundra, temperate deciduous angiosperms (Te-DA), temperate evergreen angiosperms (Te-EA), tropical evergreen angiosperms (Tr-EA), boreal evergreen gymnosperms (Br-EG), and temperate evergreen gymnosperms (Te-EG). T_{home} is the mean (1960–1996) growing season air temperature (i.e., mean temperature of the months with mean temperatures above 0°C) [Colour figure can be viewed at wileyonlinelibrary.com]

The instantaneous temperature response of the TPU rate of mature plants growing in their native environments showed distinctly different patterns among the different PFTs. Arctic tundra species showed an exponential increase in *TPU* with increasing leaf temperature, with no optimum temperature within the measured leaf temperature range (Figure 5a). All other PFTs showed a peaked response, where the rate increased up to an optimum temperature and then declined with increasing leaf temperature (Figure 5b–f). The highest optimum temperature for *TPU* was observed for tropical evergreen angiosperms (34.7°C) and the lowest was observed for the boreal evergreen gymnosperms (28.0°C). The optimum temperatures for temperate evergreen gymnosperms and temperate evergreen angiosperms were 32.5°C and 32.2°C, respectively (Table 2). The temperature response curves of *TPU* showed a significant departure from the temperature response curves of V_{cmax} (Figure S2). The rate of increase of *TPU* with temperature was shallower than that of V_{cmax} (see Figure S2), so the estimated activation energy of *TPU* was lower than that of V_{cmax} (Table 2). More importantly, in Arctic tundra, both *TPU* and V_{cmax} increased exponentially with leaf temperature and did not show a temperature optimum within the measurement leaf temperature range (Figure S2a). For other PFTs, the optimum temperature for *TPU* was approximately 6–8°C lower than that for V_{cmax} (Figure S2b–f).

The data showed a significant negative relationship between the basal rate of TPU at a standard temperature of 25°C (TPU_{25}) and the long-term mean growing season temperature of the plants' native growth environment (Figure 6a). The highest TPU_{25} was observed for Arctic tundra (30.3 ± 1.6 µmol m^{-2} s^{-1}) and the lowest for tropical evergreen angiosperms (4.7 ± 0.7 µmol m^{-2} s^{-1}). The ratio between TPU_{25} and the maximum rate of RuBP carboxylation at a standard temperature of 25°C (TPU_{25}:V_{cmax25}) also showed a decreasing trend with increasing long-term mean growing season temperature (T_{home}). Similar to TPU_{25}, the TPU_{25}:V_{cmax25} ratio was highest for the Arctic plants (Figure 6b and Table 2). We developed a simple function to implement this pattern in TBMs (Equation 7, $r^2 = .70$). Taken together, these results suggested that the net photosynthetic rate of plants in cold environments is not more frequently *TPU* limited than plants in warmer environments, as the *TPU* is higher for plants in cold environments.

$$\frac{T_{p25}}{V_{cmax25}} = 0.20 - 0.005T_{home}. \quad (7)$$

4 | DISCUSSION

Our comprehensive analysis of a global data set of plant photosynthetic CO_2 response measurements across many ecosystems, spanning a measurement temperature range of 3°C to 50°C, demonstrates that photosynthesis is not *TPU* limited at current ambient atmospheric CO_2 concentrations. We found no relationship between *TPU* limitation and leaf temperature and there was no evidence to support the view that plants growing in cold environments are more frequently *TPU* limited compared with plants growing in warmer climates. Furthermore, our analysis did not support the common assumption that *TPU* has the same temperature response function as V_{cmax}.

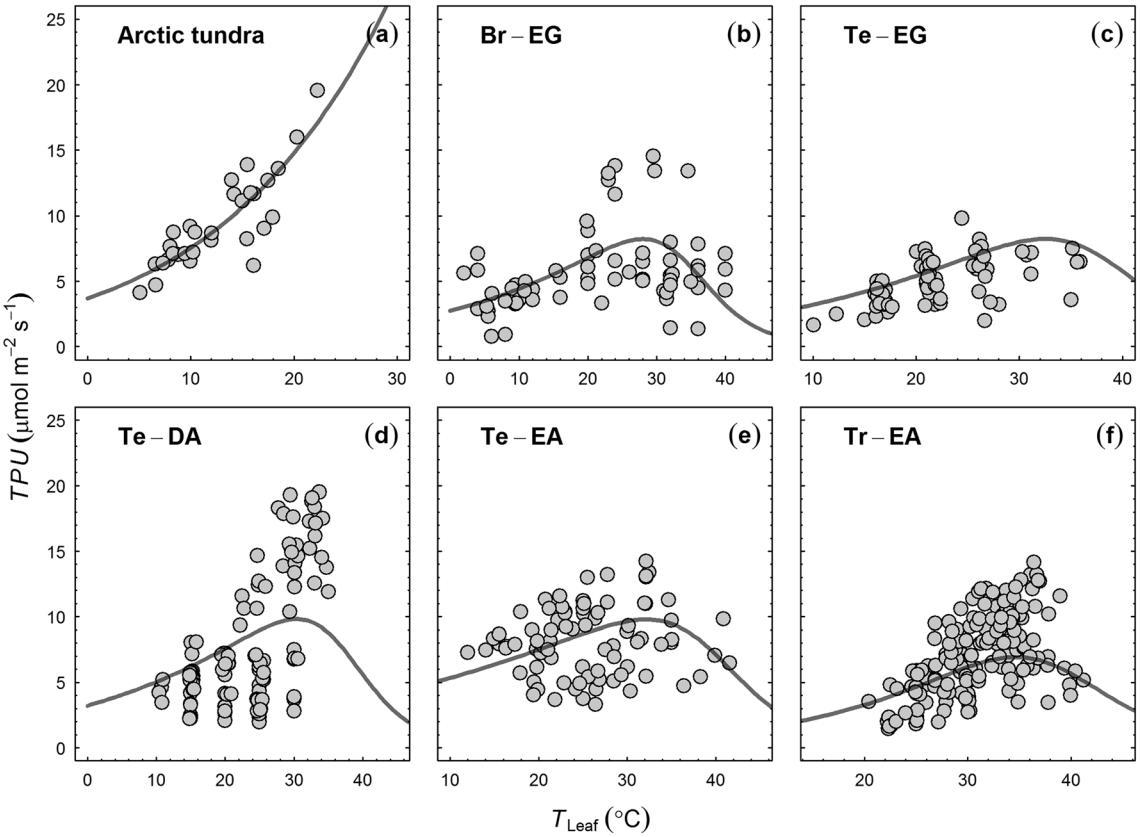

FIGURE 5 Instantaneous temperature response of the triose phosphate utilization (*TPU*) rate of mature plants growing in their native environments for different plant functional types: (a) Arctic tundra, (b) boreal evergreen gymnosperms (Br-EG), (c) temperate evergreen gymnosperms (Te-EG), (d) temperate deciduous angiosperms (Te-DA), (e) temperate evergreen angiosperms (Te-EA), and (f) tropical evergreen angiosperms (Tr-EA). Filled circles depict the *TPU* values from fitting Equation (4) to A/C_i curves (only A/C_i curves that showed *TPU* limitation within the measurement C_i range, n = 1,114). Lines in each panel show the fitted standard Arrhenius model (in Panel a) or the peaked Arrhenius model (in Panels b–f). Fitted temperature response parameters are given in Table 2. Note the disparity in x-axis scales

TABLE 2 Temperature response parameters of *TPU* and V_{cmax} for mature plants growing in their native environments

	Basal rate at 25°C (μmol m^{-2} s^{-1})		E_a (kJ mol^{-1})		ΔS (J mol^{-1} K^{-1})		T_{opt} (°C)	
Plant functional type	***TPU***	V_{cmax}	***TPU***	V_{cmax}	***TPU***	V_{cmax}	***TPU***	V_{cmax}
Arctic tundra	20.3 (1.6)	78.3 (12.7)	46.2 (5.3)	55.9 (4.8)	Not estimated	657.5 (5.7)	Not estimated	26.7
Boreal evergreen gymnosperms	7.9 (1.4)	80.4 (8.0)	30.9 (10.4)	50.3 (4.7)	650 (3.8)	637.6 (3.2)	28.0	36.1
Temperate evergreen gymnosperms	6.0 (0.9)	42.8 (13.9)	36.5 (5.6)	60.1 (7.7)	642 (4.1)	635.2 (5.6)	32.5	38.3
Temperate deciduous angiosperms	9.0 (2.1)	39.0 (1.4)	28.8 (10.6)	69.0 (3.8)	644 (3.1)	636.6 (1.7)	30.4	38.4
Temperate evergreen angiosperms	8.7 (1.0)	82.9 (11.0)	23.7 (6.1)	86.4 (4.6)	638 (3.1)	632.4 (1.7)	32.2	39.5
Tropical evergreen angiosperms	4.7 (0.7)	39.4 (8.9)	53.9 (13.8)	47.4 (10.0)	641 (3.5)	623.1 (9.1)	34.7	44.3

Note. *TPU* is the triose phosphate utilization rate, V_{cmax} is the maximum rate of RuBP carboxylation, E_a is the activation energy, ΔS is the entropy, and T_{opt} is the optimum temperature. Except for Arctic tundra, a peaked Arrhenius model was used to parameterize the instantaneous temperature response. For Arctic tundra, *TPU* exponentially increased within the measurement leaf temperature range; hence, the standard Arrhenius model was fitted to the data.

In this study, we demonstrated that light-saturated photosynthesis at current ambient atmospheric CO_2 concentrations (~400 μmol mol^{-1}) is most often Rubisco limited (80% of the A/C_i curves in our data set), which agrees with previous work demonstrating that the light-saturated photosynthetic rate at current ambient CO_2 concentration is principally limited by RuBP carboxylation (De Kauwe et al., 2016; Rogers & Humphries, 2000; Yamaguchi et al., 2016). None of the A/C_i curves included in our analysis showed a transition to the *TPU*-limited photosynthetic rate at C_i values less than or equal to 280 μmol mol^{-1}. We can, therefore, be confident that *TPU* rarely limits leaf photosynthesis in natural ecosystems at current ambient atmospheric CO_2 concentrations. Previous work has also shown that *TPU* is rarely reported as a limiting factor for leaf photosynthesis when it is measured under the ambient CO_2 and growth

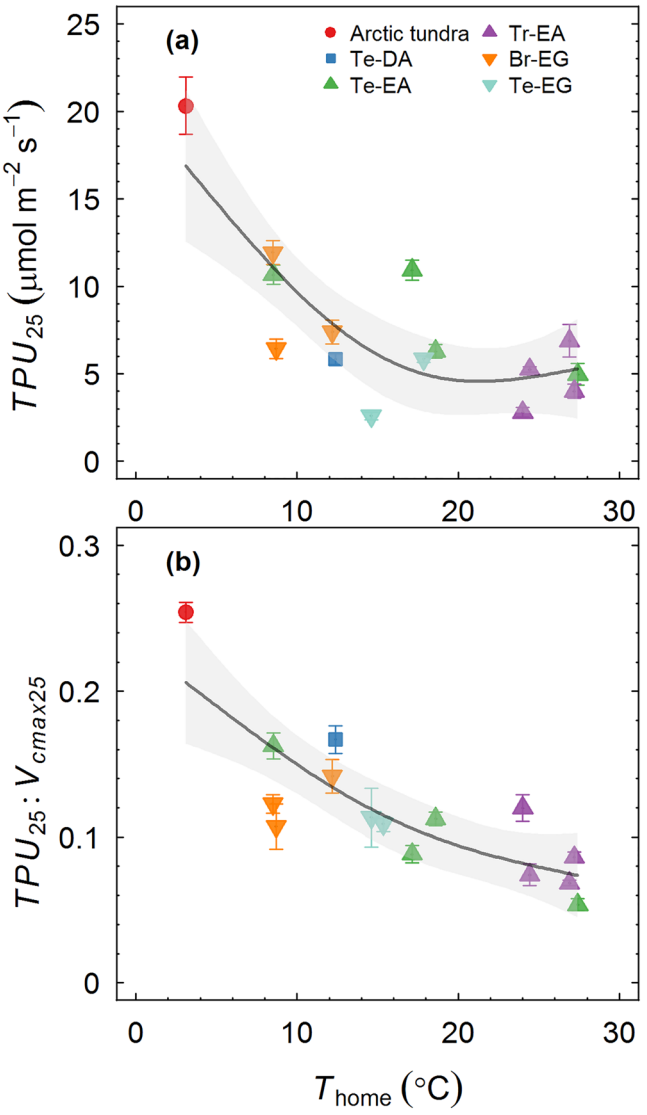

FIGURE 6 Rate of triose phosphate utilization at a standard temperature of 25°C (TPU_{25}; Panel a) and the TPU_{25}:V_{cmax25} ratio of mature plants growing in their native environments. Lines in each panel show fitted generalized additive models. Shaded area shows the 95% confidence interval of predictions. Legend in Panel (a) depicts plant functional types: Arctic tundra, temperate deciduous angiosperms (Te-DA), temperate evergreen angiosperms (Te-EA), tropical evergreen angiosperms (Tr-EA), boreal evergreen gymnosperms (Br-EG), and temperate evergreen gymnosperms (Te-EG). T_{home} is the mean (1960–1996) growing season air temperature (i.e., mean temperature of the months with mean temperatures above 0°C) at species' growing environment. Error bars represent ±1SE [Colour figure can be viewed at wileyonlinelibrary.com]

temperatures (Sage & Sharkey, 1987; Sharkey, 1985; Yang et al., 2016). Previous studies suggested that plants regulate *TPU* at a rate just slightly higher than what is likely to be required (Yang et al., 2016), but our study indicates that *TPU* limitation is unlikely to be important until CO_2 concentrations reach ~800 µmol mol^{-1}. Further, it has been reported that the *TPU* limitation usually occurs in conditions that are typical for RuBP regeneration-limited photosynthesis (Bernacchi et al., 2013). At biologically relevant leaf temperatures (~1–50°C), RuBP regeneration limitation typically occurs at higher CO_2 partial pressures and mostly at low light levels (von Caemmerer, 2000). Therefore, we conclude that it is rare for photosynthesis to be *TPU* limited under current ambient atmospheric CO_2 concentrations. Furthermore, free-air CO_2 enrichment experiments where plants are grown at elevated CO_2 concentration in field conditions have demonstrated that V_{cmax} is typically reduced at elevated CO_2 concentration, maintaining Rubisco limitation of light-saturated assimilation at elevated CO_2 (Ainsworth & Rogers, 2007). Therefore, it is highly unlikely for photosynthesis to be *TPU* limited under future predicted atmospheric CO_2 concentrations until very high levels are reached.

At low temperatures, the solubility of CO_2 and the specificity of Rubisco for CO_2 relative to O_2 increase, meaning that photorespiration decreases (Jordan & Ogren, 1984). Therefore, the capacity for regeneration of inorganic phosphate (P_i) through photorespiratory metabolism in the chloroplast is decreased because glycolate export from chloroplasts to the peroxisome is reduced (Ellsworth et al., 2015; Harley & Sharkey, 1991; Sharkey, 1985). Additionally, as enzymatic reaction rates associated with the sucrose synthesis are limited at low temperatures (Lambers et al., 2008), accumulation of triose phosphate and phosphoglyceric acid (PGA) in the chloroplast can reduce the regeneration of P_i (Ellsworth et al., 2015; Sharkey, 1985). Hence, it can be hypothesized that net photosynthetic rate could potentially be *TPU* limited in plants grown at low growth temperatures (Labate & Leegood, 1988; Lombardozzi et al., 2018; Sharkey, 2016). However, the data presented here clearly refute this hypothesis. We found a significant negative relationship between the basal rate of TPU at a standard temperature of 25°C and the long-term mean growing season temperature of the plants' native growth environment. Our data indicate that photosynthesis of plants in cold environments is not more frequently TPU limited than plants in warmer environments, as the TPU is higher for plants in cold environments.

Furthermore, there is evidence that plants have the capacity to compensate for the low temperature-induced decrease in enzyme activity associated with the Calvin cycle, electron transport, and sucrose synthesis through several mechanisms including increased concentration of photosynthetic enzymes (Yamori et al., 2005, Yamori et al., 2011), increased expression of cold stable isozymes (Yamori et al., 2006), and maintenance of membrane fluidity (Falcone, Ogas, & Somerville, 2004). Several studies provide evidence for increased concentrations of enzymes associated with sucrose synthesis, including sucrose phosphate synthase and cytosolic fructose-1,6-bisphosphatase (Strand et al., 1997; Strand et al., 1999). These mechanisms may allow cold temperature acclimation of metabolism to alleviate the *TPU* limitation to leaf photosynthesis. Additionally, cold acclimation typically increases the ratio of J_{max}:V_{cmax} (Kattge & Knorr, 2007; Kumarathunge et al., 2019; Rogers, Serbin, et al., 2017), such that the photosynthetic rate is more likely to be limited by RuBP carboxylation in cold environments. Our data showed that the C_i at the rate transition points from Rubisco carboxylation limitation to RuBP regeneration limitation was higher than the C_i values corresponding to current ambient CO_2 concentrations for Arctic species. Hence, it

is likely that the photosynthetic rate of Arctic species is most frequently RuBP carboxylation limited. Furthermore, Arctic plants have been shown to have a large root to shoot ratio (Iversen et al., 2015), suggesting that sink strength may be sufficient to enable high rates of sucrose export from the leaf and avoid *TPU* limitation (McClain & Sharkey, 2019).

We observed lower activation energies for the instantaneous temperature response of *TPU* compared with V_{cmax} for most PFTs, contradicting the common assumption of similar temperature responses for both processes. Our results contrast with the previous finding by Yang et al. (2016), who reported higher temperature sensitivity of *TPU* compared with V_{cmax}. The activation energies reported in this study were relatively low compared with the values reported by Yang et al. (2016). The temperature response parameters in Yang et al. (2016) were derived using *TPU* data from different studies where the method of calculating *TPU* (e.g., kinetic constants used in calculations) was not consistent among studies. Hence, our parameter estimates are not directly comparable with those of Yang et al. (2016). Moreover, our results indicate distinct patterning in the basal rate of *TPU* measured at a standard temperature (TPU_{25}) across a climate gradient of long-term mean growing season temperatures. Both TPU_{25} and TPU_{25}:V_{cmax25} were higher for plants growing in cold environments compared with plants in warm environments. The observed pattern for TPU_{25}:V_{cmax25} with T_{home} is consistent with the pattern observed for J_{max}:V_{cmax} at a standard temperature of 25°C at the global scale (Kumarathunge et al., 2019). Taken together, these results suggest that the use of the temperature response function of V_{cmax} to model the temperature response of *TPU*, as implemented in several TBMs, is not correct. Further, our finding of a temperature dependence challenges the use of fixed *TPU*:V_{cmax} ratio in TBMs (Clark et al., 2011; Collatz et al., 1991; Lombardozzi et al., 2018).

Our data demonstrate that the modelled effects of *TPU* limitation on global terrestrial GPP and the global carbon cycle may not be as large as reported by Lombardozzi et al. (2018), either at current or future projected atmospheric CO_2 concentrations. Lombardozzi et al. (2018) assumed a fixed *TPU*:V_{cmax} ratio, but here, we demonstrated that the *TPU*:V_{cmax} ratio decreases with increasing temperature. Further, photosynthetic acclimation to rising CO_2 concentration is not currently implemented in the model used in their study (i.e., CLM4.5). Hence, it is likely that CLM predicts a higher sensitivity to *TPU* at future CO_2 concentrations that is not supported by observations (Ainsworth & Rogers, 2007; Leakey et al 2009). We recommend that TBMs should dynamically change *TPU*:V_{cmax} with plants' growth temperature and should use separate temperature response functions to characterize the temperature dependency of *TPU*. Further, it is necessary to implement photosynthetic acclimation to rising CO_2 concentration in TBMs to improved predictions of GPP in high CO_2 model simulations.

Our global scale synthesis of leaf photosynthesis using measurements obtained from a large number of studies, species, plant functional types, and a wide temperature range reveals that the extent of *TPU* limitation at the global scale is uncommon and unrelated to temperature of the growing environment. Taken together, our new formulations of the temperature response of *TPU* should prove useful in quantifying the biochemical limits of terrestrial plant photosynthesis and improving the representation of plant photosynthesis in TBMs.

ACKNOWLEDGMENTS

D.K. was supported by a Western Sydney University International PhD Scholarship. A.R. was supported by the Next-Generation Ecosystem Experiments (NGEE Arctic) project that is supported by the Office of Biological and Environmental Research in the Department of Energy, Office of Science, and through the United States Department of Energy contract no. DE-SC0012704 to Brookhaven National Laboratory. We thank all data contributors for their valuable contribution. We thank Tom Sharkey and an anonymous reviewer for their comments, which served to improve the manuscript.

AUTHOR CONTRIBUTIONS

The project was conceived and led by B.E.M. The analyses were designed and carried out by D.P.K. with guidance from B.E.M. Manuscript writing was led by D.P.K. and B.E.M. J.E.D., A.R., and M.G.T. made substantial contributions to the data interpretation and writing.

ORCID

Dushan P. Kumarathunge https://orcid.org/0000-0003-1309-4731
Belinda E. Medlyn https://orcid.org/0000-0001-5728-9827
John E. Drake https://orcid.org/0000-0001-9453-1766
Alistair Rogers https://orcid.org/0000-0001-9262-7430
Mark G. Tjoelker https://orcid.org/0000-0003-4607-5238

REFERENCES

Ainsworth, E. A., & Rogers, A. (2007). The response of photosynthesis and stomatal conductance to rising [CO_2]: Mechanisms and environmental interactions. *Plant, Cell & Environment*, *30*(3), 258–270. https://doi.org/10.1111/j.1365-3040.2007.01641.x

Bahar, N. H. A., Hayes, L., Scafaro, A. P., Atkin, O. K., & Evans, J. R. (2018). Mesophyll conductance does not contribute to greater photosynthetic rate per unit nitrogen in temperate compared with tropical evergreen wet-forest tree leaves. *New Phytologist*, *218*, 492–505. https://doi.org/10.1111/nph.15031

Bernacchi, C. J., Bagley, J. E., Serbin, S. P., Ruiz-Vera, U. M., Rosenthal, D. M., & Vanloocke, A. (2013). Modelling C3 photosynthesis from the chloroplast to the ecosystem. *Plant, Cell & Environment*, *36*(9), 1641–1657. https://doi.org/10.1111/pce.12118

Bernacchi, C. J., Singsaas, E. L., Pimentel, C., Portis, A. R. Jr., & Long, S. P. (2001). Improved temperature response functions for models of Rubisco-limited photosynthesis. *Plant, Cell & Environment*, *24*(2), 253–259. https://doi.org/10.1111/j.1365-3040.2001.00668.x

Busch, F. A., & Sage, R. F. (2017). The sensitivity of photosynthesis to O_2 and CO_2 concentration identifies strong Rubisco control above the thermal optimum. *New Phytologist*, *213*(3), 1036–1051. https://doi.org/10.1111/nph.14258

Clark, D. B., Mercado, L. M., Sitch, S., Jones, C. D., Gedney, N., Best, M. J., … Cox, P. M. (2011). The Joint UK Land Environment Simulator (JULES), model description–part 2: Carbon fluxes and vegetation dynamics. *Geoscientific Model Development*, *4*(3), 701–722. https://doi.org/10.5194/gmd-4-701-2011

Collatz, G. J., Ball, J. T., Grivet, C., & Berry, J. A. (1991). Physiological and environmental regulation of stomatal conductance, photosynthesis and transpiration: A model that includes a laminar boundary layer. *Agricultural and Forest Meteorology*, *54*(2), 107–136. https://doi.org/10.1016/0168-1923(91)90002-8

Crous, K. Y., Quentin, A. G., Lin, Y. S., Medlyn, B. E., Williams, D. G., Barton, C. V., & Ellsworth, D. S. (2013). Photosynthesis of temperate *Eucalyptus globulus* trees outside their native range has limited adjustment to elevated CO_2 and climate warming. *Glob Chang Biol*, *19*(12), 3790–3807. https://doi.org/10.1111/gcb.12314

De Kauwe, M. G., Lin, Y.-S., Wright, I. J., Medlyn, B. E., Crous, K. Y., Ellsworth, D. S., … Domingues, T. F. (2016). A test of the 'one-point method' for estimating maximum carboxylation capacity from field-measured, light-saturated photosynthesis. *New Phytologist*, *210*(3), 1130–1144. https://doi.org/10.1111/nph.13815

Dreyer, E., Le Roux, X., Montpied, P., Daudet, F. A., & Masson, F. (2001). Temperature response of leaf photosynthetic capacity in seedlings from seven temperate tree species. *Tree Physiology*, *21*(4), 223–232. https://doi.org/10.1093/treephys/21.4.223

Duursma, R. A. (2015). Plantecophys—An R package for analysing and modelling leaf gas exchange data. *PLoS ONE*, *10*(11), e0143346. https://doi.org/10.1371/journal.pone.0143346

Ellsworth, D. S., Crous, K. Y., Lambers, H., & Cooke, J. (2015). Phosphorus recycling in photorespiration maintains high photosynthetic capacity in woody species. *Plant, Cell & Environment*, *38*(6), 1142–1156. https://doi.org/10.1111/pce.12468

Falcone, D. L., Ogas, J. P., & Somerville, C. R. (2004). Regulation of membrane fatty acid composition by temperature in mutants of Arabidopsis with alterations in membrane lipid composition. *BMC Plant Biology*, *4*(1), 17. https://doi.org/10.1186/1471-2229-4-17

Farquhar, G. D., von Caemmerer, S., & Berry, J. A. (1980). A biochemical model of photosynthetic CO_2 assimilation in leaves of C3 species. *Planta*, *149*(1), 78–90. https://doi.org/10.1007/BF00386231

Gu, L., Pallardy, S. G., Tu, K., Law, B. E., & Wullschleger, S. D. (2010). Reliable estimation of biochemical parameters from C_3 leaf photosynthesis–intercellular carbon dioxide response curves. *Plant, Cell & Environment*, *33*(11), 1852–1874. https://doi.org/10.1111/j.1365-3040.2010.02192.x

Harley, P. C., & Sharkey, T. D. (1991). An improved model of C_3 photosynthesis at high CO_2: Reversed O_2 sensitivity explained by lack of glycerate re-entry into the chloroplast. *Photosynthesis Research*, *27*(3), 169–178.

Hijmans, R. J., Cameron, S. E., Parra, J. L., Jones, P. G., & Jarvis, A. (2005). Very high resolution interpolated climate surfaces for global land areas. *International Journal of Climatology*, *25*(15), 1965–1978. https://doi.org/10.1002/joc.1276

Hikosaka, K., Ishikawa, K., Borjigidai, A., Muller, O., & Onoda, Y. (2006). Temperature acclimation of photosynthesis: Mechanisms involved in the changes in temperature dependence of photosynthetic rate. *Journal of Experimental Botany*, *57*(2), 291–302. https://doi.org/10.1093/jxb/erj049

Iversen, C. M., Sloan, V. L., Sullivan, P. F., Euskirchen, E. S., McGuire, A. D., Norby, R. J., … Wullschleger, S. D. (2015). The unseen iceberg: Plant roots in arctic tundra. *New Phytologist*, *205*(1), 34–58. https://doi.org/10.1111/nph.13003

Johnson, F. H., Eyring, H., & Williams, R. W. (1942). The nature of enzyme inhibitions in bacterial luminescence: Sulfanilamide, urethane, temperature and pressure. *Journal of Cellular and Comparative Physiology*, *20*, 247–268. https://doi.org/10.1002/jcp.1030200302

Jordan, D. B., & Ogren, W. L. (1984). The CO_2/O_2 specificity of ribulose 1,5-bisphosphate carboxylase/oxygenase. *Planta*, *161*(4), 308–313. https://doi.org/10.1007/BF00398720

Kattge, J., & Knorr, W. (2007). Temperature acclimation in a biochemical model of photosynthesis: A reanalysis of data from 36 species. *Plant, Cell & Environment*, *30*(9), 1176–1190. https://doi.org/10.1111/j.1365-3040.2007.01690.x

Kattge, J., Knorr, W., Raddatz, T., & Wirth, C. (2009). Quantifying photosynthetic capacity and its relationship to leaf nitrogen content for global-scale terrestrial biosphere models. *Global Change Biology*, *15*(4), 976–991. https://doi.org/10.1111/j.1365-2486.2008.01744.x

Kumarathunge, D. P., Medlyn, B. E., Drake, J. E., Tjoelker, M. G., Aspinwall, M. J., Battaglia, M., … Danielle, A. W. (2018). ACi-TGlob_V1.0: A global dataset of photosynthetic CO_2 response curves of terrestrial plants. https://doi.org/10.6084/m9.figshare.7283567.v1

Kumarathunge, D. P., Medlyn, B. E., Drake, J. E., Tjoelker, M. G., Aspinwall, M. J., Battaglia, M., … Way, D. A. (2019). Acclimation and adaptation components of the temperature dependence of plant photosynthesis at the global scale. *New Phytologist*, *222*, 768–784. https://doi.org/10.1111/nph.15668

Labate, C. A., & Leegood, R. C. (1988). Limitation of photosynthesis by changes in temperature. *Planta*, *173*(4), 519–527. https://doi.org/10.1007/BF00958965

Lombardozzi, D., Nicholas, G. S., Susan, J. C., Jeffrey, S. D., Thomas, D. S., Alistair, R., … Gordon, B. B. (2018). Triose phosphate limitation in photosynthesis models reduces leaf photosynthesis and global terrestrial carbon storage. *Environmental Research Letters*, *13*(7), 074025. https://doi.org/10.1088/1748-9326/aacf68

Manter, D. K., & Kerrigan, J. (2004). A/C_i curve analysis across a range of woody plant species: Influence of regression analysis parameters and mesophyll conductance. *Journal of Experimental Botany*, *55*(408), 2581–2588. https://doi.org/10.1093/jxb/erh260

McClain, A. M., & Sharkey, T. D. (2019). Triose phosphate utilization and beyond: From photosynthesis to end product synthesis. *Journal of Experimental Botany*, *70*, 1755–1766. https://doi.org/10.1093/jxb/erz058

Medlyn, B. E., Dreyer, E., Ellsworth, D., Forstreuter, M., Harley, P. C., Kirschbaum, M. U. F., … Loustau, D. (2002). Temperature response of parameters of a biochemically based model of photosynthesis. II. A review of experimental data. *Plant, Cell & Environment*, *25*(9), 1167–1179. https://doi.org/10.1046/j.1365-3040.2002.00891.x

Medlyn, B. E., Duursma, R. A., & Zeppel, M. J. B. (2011). Forest productivity under climate change: A checklist for evaluating model studies. *Wiley Interdisciplinary Reviews: Climate Change*, *2*(3), 332–355.

Mercado, L. M., Medlyn, B. E., Huntingford, C., Oliver, R. J., Clark, D. B., Stephen, S., … Cox, P. M. (2018). Large sensitivity in land carbon storage due to geographical and temporal variation in the thermal response of photosynthetic capacity. *New Phytologist*, *218*(4), 1462–1477. https://doi.org/10.1111/nph.15100

Pons, T. L. (2012). Interaction of temperature and irradiance effects on photosynthetic acclimation in two accessions of arabidopsis thaliana. *Photosynthesis Research.*, *113*(1), 207–219. https://doi.org/10.1007/s11120-012-9756-3

Rigby, R. A., & Stasinopoulos, D. M. (2005). Generalized additive models for location, scale and shape. *Journal of the Royal Statistical Society: Series C (Applied Statistics)*, *54*(3), 507–554. https://doi.org/10.1111/j.1467-9876.2005.00510.x

Rogers, A., & Humphries, S. W. (2000). A mechanistic evaluation of photosynthetic acclimation at elevated CO2. *Global Change Biology*, *6*(8), 1005–1011. https://doi.org/10.1046/j.1365-2486.2000.00375.x

Rogers, A., Medlyn, B. E., Dukes, J. S., Bonan, G., von Caemmerer, S., Dietze, M. C., … Zaehle, S. (2017). A roadmap for improving the representation of

photosynthesis in Earth system models. *New Phytologist*, *213*(1), 22–42. https://doi.org/10.1111/nph.14283

Rogers, A., Serbin, S. P., Ely, K. S., Sloan, V. L., & Wullschleger, S. D. (2017). Terrestrial biosphere models underestimate photosynthetic capacity and CO_2 assimilation in the Arctic. *New Phytologist*, *216*(4), 1090–1103. https://doi.org/10.1111/nph.14740

Sage, R. F., & Sharkey, T. D. (1987). The effect of temperature on the occurrence of O_2 and CO_2 insensitive photosynthesis in field grown plants. *Plant Physiology*, *84*(3), 658–664. https://doi.org/10.1104/pp.84.3.658

Sage, R. F., Sharkey, T. D., & Seemann, J. R. (1989). Acclimation of photosynthesis to elevated CO_2 in five C_3 species. *Plant Physiology*, *89*(2), 590–596. https://doi.org/10.1104/pp.89.2.590

Sharkey, T. D. (1985). Photosynthesis in intact leaves of C_3 plants: Physics, physiology and rate limitations. *The Botanical Review*, *51*(1), 53–105. https://doi.org/10.1007/BF02861058

Sharkey, T. D. (2016). What gas exchange data can tell us about photosynthesis. *Plant, Cell & Environment*, *39*(6), 1161–1163. https://doi.org/10.1111/pce.12641

Sharkey, T. D., Bernacchi, C. J., Farquhar, G. D., & Singsaas, E. L. (2007). Fitting photosynthetic carbon dioxide response curves for C3 leaves. *Plant, Cell & Environment*, *30*(9), 1035–1040. https://doi.org/10.1111/j.1365-3040.2007.01710.x

Sharkey, T. D., Stitt, M., Heineke, D., Gerhardt, R., Raschke, K., & Heldt, H. W. (1986). Limitation of photosynthesis by carbon metabolism II. O_2-insensitive CO_2 uptake results from limitation of triose phosphate utilization. *Plant Physiology*, *81*, 1123–1129. https://doi.org/10.1104/pp.81.4.1123

Smith, N. G., & Dukes, J. S. (2013). Plant respiration and photosynthesis in global-scale models: Incorporating acclimation to temperature and CO_2. *Global Change Biology*, *19*(1), 45–63. https://doi.org/10.1111/j.1365-2486.2012.02797.x

Smith, N. G., Lombardozzi, D., Tawfik, A., Bonan, G., & Dukes, J. S. (2017). Biophysical consequences of photosynthetic temperature acclimation for climate. *Journal of Advances in Modeling Earth Systems*, *9*(1), 536–547. https://doi.org/10.1002/2016MS000732

Smith, N. G., Malyshev, S. L., Shevliakova, E., Kattge, J., & Dukes, J. S. (2016). Foliar temperature acclimation reduces simulated carbon sensitivity to climate. *Nature Clim. Change*, *6*(4), 407–411. https://doi.org/10.1038/nclimate2878

Stitt, M., & Grosse, H. (1988). Interactions between sucrose synthesis and CO_2 fixation IV. Temperature-dependent adjustment of the relation between sucrose synthesis and CO_2 fixation. *Journal of Plant Physiology*, *133*, 392–400. https://doi.org/10.1016/S0176-1617(88)80025-7

Stitt, M., Grosse, H., & Woo, K.-C. (1988). Interactions between sucrose synthesis and CO_2 fixation II. Alterations of fructose 2,6-bisphosphate during photosynthetic oscillations. *Journal of Plant Physiology*, *133*, 138–143. https://doi.org/10.1016/S0176-1617(88)80128-7

Stitt, M., & Hurry, V. (2002). A plant for all seasons: alterations in photosynthetic carbon metabolism during cold acclimation in Arabidopsis. *Current Opinion in Plant Biology*, *5*(3), 199–206. https://doi.org/10.1016/S1369-5266(02)00258-3

Strand, Å., Hurry, V., Gustafsson, P., & Gardeström, P. (1997). Development of *Arabidopsis thaliana* leaves at low temperatures releases the suppression of photosynthesis and photosynthetic gene expression despite the accumulation of soluble carbohydrates. *The Plant Journal*, *12*(3), 605–614. https://doi.org/10.1046/j.1365-313X.1997.00583.x

Strand, Å., Hurry, V., Henkes, S., Huner, N., Gustafsson, P., Gardeström, P., & Stitt, M. (1999). Acclimation of Arabidopsis leaves developing at low temperatures. Increasing cytoplasmic volume accompanies increased activities of enzymes in the Calvin cycle and in the sucrose-biosynthesis pathway. *Plant Physiology*, *119*(4), 1387–1398. https://doi.org/10.1104/pp.119.4.1387

Von Caemmerer, S. (2013). Steady-state models of photosynthesis. *Plant, Cell & Environment*, *36*(9), 1617–1630. https://doi.org/10.1111/pce.12098

Yang, J. T., Preiser, A. L., Li, Z., Weise, S. E., & Sharkey, T. D. (2016). Triose phosphate use limitation of photosynthesis: Short-term and long-term effects. *Planta*, *243*(3), 687–698. https://doi.org/10.1007/s00425-015-2436-8

SUPPORTING INFORMATION

Additional supporting information may be found online in the Supporting Information section at the end of the article.

Figure S1 Distribution of (a) measured maximum intercellular CO_2 concentration (C_i) of individual AC_i curves (n = 4260), (b) C_i at the current ambient CO_2 concentration of 400 μmol mol^{-1} (n = 7269) and (c) maximum atmospheric CO_2 concentration (C_a) set point of individual AC_i curves (n = 4183). In panel (a), continuous vertical line depicts the median C_i at process transition between RuBP-regeneration limited photosynthetic rate to T_P limited photosynthetic rate (M_{TPU}) and the dashed line depicts the median maximum C_i of the distribution (M). In panels (b) and (c), the dash line depicts the median (M) of the distribution. Note in some A/C_i curves, there were multiple measurements at ambient CO_2 levels. Hence the number of data points at ambient CO_2 level was higher than the number of A/C_i curves.

Figure S2 Instantaneous temperature response of the rate of triose phosphate utilisation rate (*TPU*; black) and the maximum rate of ribulose-1,5-bisphosphate carboxylase-oxygenase (Rubisco) activity (V_{cmax}; red) of mature plants growing in their native environments for different plant functional types, Arctic tundra, Boreal evergreen gymnosperms (Br-EG), Temperate evergreen gymnosperms (Te-EG), Temperate deciduous angiosperms (Te-DA), Temperate evergreen angiosperms (Te-EA), Tropical evergreen angiosperms (Tr-EA). Data shown here are the standardised to values at 25 °C.

Table S1. List of species, seed source location and measurement settings. Treatments column shows specific growth temperature, growth CO_2 concentration and watering treatments whenever implemented in different datasets. We recommend users to refer to the original publications given for each datasets for more detailed explanation on different treatments. Unless specially mentioned, plants were grown under natural light conditions. In datasets where specific treatments not implemented, plants were grown under natural environmental conditions of the experimental site

How to cite this article: Kumarathunge DP, Medlyn BE, Drake JE, Rogers A, Tjoelker MG. No evidence for triose phosphate limitation of light-saturated leaf photosynthesis under current atmospheric CO_2 concentration. *Plant Cell Environ*. 2019;42:3241–3252. https://doi.org/10.1111/pce.13639